Multi-cationic molten salt electrolyte of low-temperature sodium liquid metal battery for grid storage

Wenjin Ding[1,a*], Qing Gong[1,a*], Shengzhi Liang[1], Ralf Hoffmann[1], Hao Zhou[2], Haomiao Li[2*], Kangli Wang[2], Tianru Zhang[3], Alfons Weisenburger[3], Georg Müller[3], Alexander Bonk[1]

[1]Institute of Engineering Thermodynamics, German Aerospace Center (DLR), Stuttgart, Germany

[2]School of Electrical and Electronic Engineering, Huazhong University of Science and Technology (HUST), Wuhan, China

[3]Institute for Pulsed Power and Microwave Technology, Karlsruhe Institute of Technology (KIT), Eggenstein-Leopoldshafen, Germany

[a]Co-first authors: W. Ding and Q. Gong contributed equally to this work.

*Corresponding authors:

W. Ding (Tel.: +49 711 6862-233, Email: wenjin.ding@dlr.de)

Q. Gong (Tel.: +49 711 6862-8417, Email: qing.gong@dlr.de)

H. Li (Tel.: +86 027 8755-9524, Email: lihm@hust.edu.cn)

ABSTRACT

Multi-cationic molten chloride salt mixtures such as LiCl-KCl-NaCl are promising molten salt electrolytes for low-temperature (≤450°C) sodium liquid metal batteries (Na-LMBs) due to their low melting temperatures. In this work, the melting temperatures of the LiCl-KCl-NaCl ternary mixtures were determined with Differential Scanning Calorimetry (DSC), assisted by the simulation software FactSage™ and confirmed by a melting point apparatus OptiMelt™. It is founded that the eutectic LiCl-KCl-NaCl can be considered as a pseudo-binary system with LiCl-KCl eutectic (59.2-40.8 mol.%) as the solvent and NaCl as the solute. When the molar fraction of NaCl is not more than 9 mol.%, the eutectic LiCl-KCl-NaCl salt mixture has a similar melting temperature of about 350°C as that of LiCl-KCl eutectic. In addition, the exchange reactions between anode Na metal with LiCl-KCl-NaCl molten salt electrolyte were studied at the temperature of 400 °C, 450 °C, and 500 °C quantitatively. The equilibrium constants of the exchange reactions were determined by chemical analysis on the salt and metal phases by Ion Chromatography (IC). A one ampere-hour (Ah) Na-LMB test cell based on the findings in this work was built and shows promising energy storage performance. Moreover, the phenomena in the cell test can be explained convincingly, combining the results of exchange reactions and the

pseudo-binary-system theory. The findings on the multi-cationic molten salt electrolyte in this work could support further development of the liquid metal batteries.

Keywords: Grid storage; Liquid metal battery (LMB); LiCl-KCl-NaCl molten salt electrolyte; Pseudo-binary system; Melting temperature; Exchange reaction.

1. INTRODUCTION

Liquid metal batteries (LMBs) are perceived as one kind of the most promising batteries for large-scale grid storage due to their cost-effectiveness (~30 $/kWh), excellent stability (>10 000 cycles), high energy storage efficiency (>70 %) and high safety [1-3]. LMBs could be Mg-based [4], Li-based [3, 5-8], Ca-based [9, 10], Na-based [1, 11, 12], etc. with difference metals as the anode. Among them, the Ca-based LMB of Ambri (a start-up of MIT) has been pre-commercial. In 2019, Ambri received an investment of $144 million from Reliance Industries of Bill Gates to build manufacturing facilities in order to meet growing grid storage demand [13].

Increasing attention is paid to Na-LMBs because of the abundance and low material cost of Na (compared to Li) as well as the low melting temperature of Na metal (T_m= 98°C, compared to Ca and Mg metals) for potential low cell operating temperatures. However, most Na-LMBs available in the literature have high operating temperatures (>550°C) since they use single-cationic halide salt mixtures with high melting temperatures (e.g., NaF-NaCl-NaI with a eutectic melting temperature of 530°C) [14]. Thus, their self-discharge rates caused by the high solubility of Na metal in the molten salt electrolyte at high temperatures are unacceptably high [14]. For instance, the Na-Bi test LMB-cell with the NaF-NaCl-NaI electrolyte, which was tested by Argonne National Laboratory (ANL), had an operating temperature of 580°C and showed that its Coulombic and energy efficiency was less than 80% and 60%, respectively [14]. Additionally, the high operating temperature of Na-LMB could lead to other technical challenges for its large-scale commercial applications, such as severe corrosion of metallic structural materials, high-temperature heat management, and high Na vapor pressure [15].

As electrolytes for LMBs, molten halide salts are remarkable and promising because of their high thermal/chemical stability, high electrical and ionic conductivity, and low costs [3, 4, 9, 12, 16]. As discussed in our previous work [16] [17], multi-cationic electrolytes (e.g., LiCl-NaCl-KCl) for Na-based LMBs can reduce the melting temperature (i.e., the operating temperature) and the solubility of Na-anode in the electrolyte (i.e., the self-discharge) in parallel, leading to a significant improvement of battery performance. In our previous work [16], we investigated the Na-LMBs using the LiCl-NaCl-KCl multi-cationic electrolyte with an operating temperature of 450°C [17]. The Na| LiCl-NaCl-KCl (59:5:36 mol%, melting temperature of about 350°C) |Bi_9Sb cells reach an energy efficiency of approximately 80 %, a Coulombic efficiency of >97 %, and neglectable capacity loss after 700 cycles at 450 °C (estimated > 15 000 cycles in lifetime). However, the test

cell using eutectic LiCl-NaCl-KCl with 9 mol% NaCl (with a melting temperature of about 350°C) showed worse cell performance than that using 5 mol% NaCl, although the higher concentration of NaCl increases the Na^+ conductivity. The LMB research group in Helmholtz-Zentrum Dresden-Rossendorf (HZDR) in Germany also reported the poor cell performance of the Na-LMB using eutectic LiCl-NaCl-KCl with 9 mol% NaCl [12]. These studies focus on the battery tests, not on the molten salt electrolyte. However, it is a crucial part of the LMB and there is a lack of knowledge (e.g., interaction of molten salt electrolytes with the metal electrodes) on the molten salt electrolyte, particularly on the multi-cationic molten salt electrolyte. Thus, this work will have a deep study on the multi-cationic molten salt electrolyte for improving the storage performance of the Na-LMB.

The phase diagram of the LiCl-KCl binary system in Fig. 1 shows that the eutectic composition is 59.2 mol.% LiCl-40.8 mol.% KCl with the melting temperature of 353 °C [18, 19]. In the nuclear and rare earth industry [20, 21], the LiCl-KCl eutectic ((LiCl-KCl)eut.) binary system is used as a low-melting-point molten chloride solvent. Other chlorides (e.g., UCl_3, $LnCl_3$) dissolve in the (LiCl-KCl)eut. with little change in the melting point. This MClx-(LiCl-KCl)eut. ternary system was called pseudo-binary system [20, 22, 23], in which (LiCl-KCl)eut. and MClx were seen as a solvent and solute, respectively. In the published phase diagrams of LiCl-KCl-NaCl shown in Fig. 2, NaCl-(LiCl-KCl)eut. also showed the pseudo-binary characteristics [20]. However, there are some controversies about the eutectic temperature and composition of the LiCl-NaCl-KCl ternary system in the published literature, as shown in **Table 1**, indicating that the study of the LiCl-KCl-NaCl is still not sufficient. Hence, the study on the phase diagram of the NaCl-LiCl-KCl ternary system in this work was converted to 1). the solubility of NaCl in (LiCl-KCl)eut. at the melting point of this binary system, and 2). variation of the solubility of NaCl in (LiCl-KCl)eut. with temperatures higher than the melting point of this binary system.

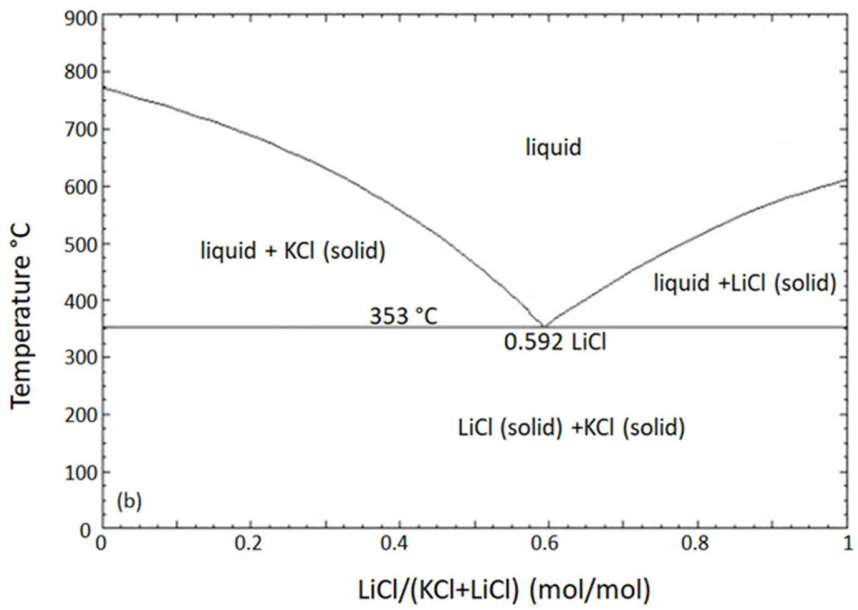

Fig. 1. Phase diagram of LiCl-KCl binary system simulated by FactSage.

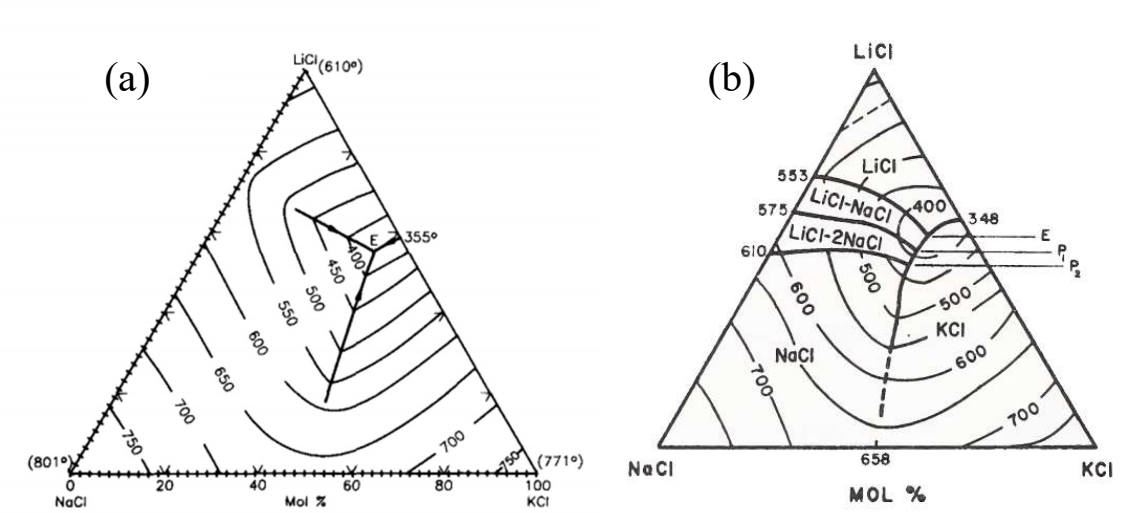

Fig. 2. (a) Simulated phase diagram of LiCl-KCl-NaCl in 1991 [24]; (b) Experimental phase diagram of LiCl-KCl-NaCl in 1979 [25].

Table 1. Melting points and salt compositions (in mol%) of eutectic LiCl-KCl-NaCl in literature.

Data sources	LiCl	KCl	NaCl	Melting temperature °C
[24]	55	36	9	343
[26]	49	33.7	17.3	333
[27]	54	33.4	12.6	348

For membrane-free LMBs, it is essential to consider the compatibility between the electrodes and electrolytes. The multi-cationic electrolytes can mitigate the problem of high solubility of the anode metal in the electrolyte by reducing operating temperature of the cell [9, 16, 17]. However, different from the single-cationic electrolytes, exchange reactions between the multi-cationic electrolytes and the anode metals (as shown in **Eq. 1**) are needed to be studied since the exchange reactions could significantly change the compositions of the electrolytes and anode metals, and their properties.

Exchange reaction: A (anode metal) + B^+ (ion in molten salt) ↔ A^+ + B **Eq. 1**

In the available literature on LMBs, less attention has been paid to the exchange reactions between the anode metal and molten salt electrolyte. Most published LMBs used single-cationic halide salt mixtures such as NaF-NaCl-NaI [14], which could avoid the problem of exchange reactions between anode and electrolyte [1, 3]. However, such exchange reaction has been discovered and studied in Li-LMB using multi-cationic molten salt electrolyte [7, 8]. Blanchard [8] reported the potential reaction between KCl and Li to be LiCl and K at 500 °C, even when KCl has a lower Gibbs free energy of formation ($\Delta_f G^\circ$) than that of LiCl at 500 °C. However, its influence on the cell performance was not studied in-depth. Similarly, the exchange reactions between Na-metal and Li^+/K^+ at operating temperature should be studied for Na-based LMBs with LiCl-KCl-NaCl electrolyte. To our best knowledge, there is less study available in the literature on the exchange reactions of Na-metal with molten LiCl-KCl-NaCl and their effect on the cell performance.

In this work, LiCl-KCl-NaCl as the electrolyte of Na-LMBs was systematically studied as shown in Fig. 3. Firstly, the eutectic salt composition and the melting point of LiCl-KCl-NaCl were estimated with thermodynamic simulation via FactSage™ software (Step 1), then verified with the thermal analysis via Differential Scanning Calorimetry (DSC) and a melting point apparatus (OptiMelt™) (Step 2). The results were used to suggest the operating temperatures and the molten salt electrolyte composition of the LMB cell. After that, the exchange reactions between Na-metal and molten LiCl-KCl-NaCl were studied via Ion Chromatography (IC) in Step 3. The equilibrium constants (K_{eq}) of the exchange reactions of Na-metal with Li^+ and K^+ were determined based on the IC data. Finally, based on the findings on the LiCl-KCl-NaCl electrolyte, a one ampere-hour (Ah) Na||Bi_9Sb battery test was built and tested to investigate the influence of the exchange

reactions on the cell performance (Step 4). This work is expected to develop a method with experiments and simulations on multi-cationic molten salt electrolytes to support further development of their applications in the liquid metal batteries.

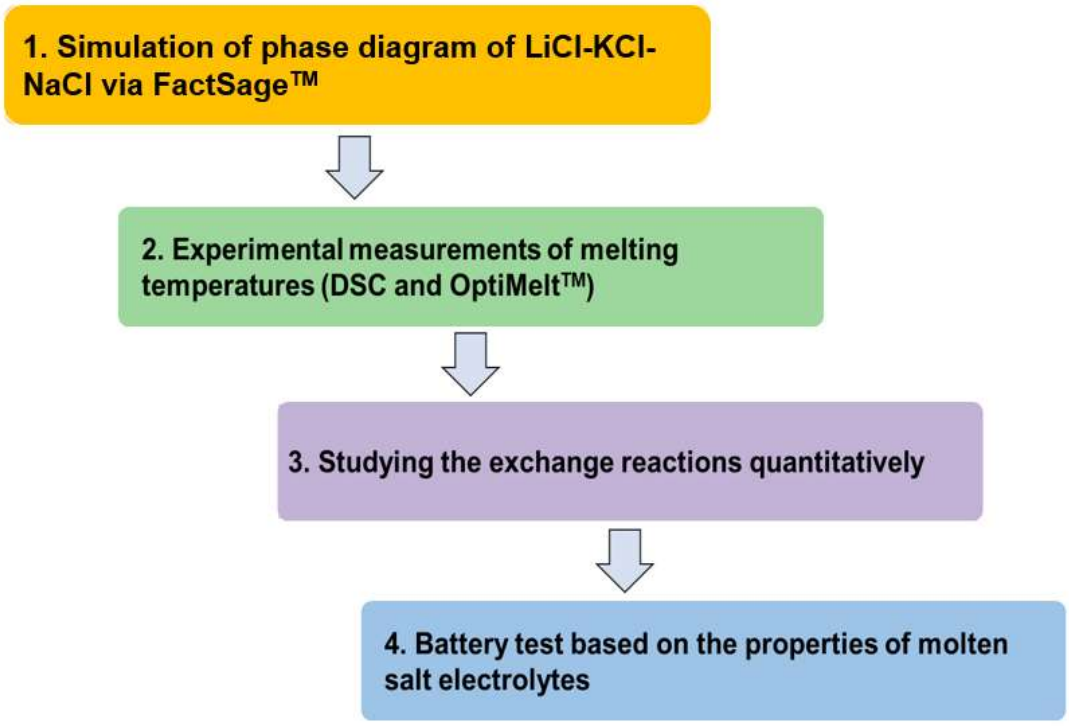

Fig. 3 Flowchart of investigation on multi-cationic molten salt electrolyte for Na-LMB in this work.

2. MATERIAL AND METHODS

2.1 Melting temperature of LiCl-KCl-NaCl

Three methods were employed to determine the eutectic salt compositions and melting points of LiCl-KCl-NaCl, including FactSage™ [28] simulation, differential scanning calorimetry (DSC), and OptiMelt™. Firstly, the melting points of LiCl-KCl-NaCl were simulated by FactSage™. More details on the FactSage simulation for molten salts could be found in our previous work [16]. Secondly, the melting points of six salts with different NaCl mol.% (as shown in **Table 2**), which were selected based on the FactSage simulation, were verified by DSC. Among these salts, the ratio of LiCl and KCl was fixed to the eutectic ratio of 59.2-40.8 mol.%, while the amount of NaCl ranged from 0 to 19 mol.% of the total. The salts with different compositions are written as (LiCl-KCl)eut.-xNaCl, where x is from 0 to 19 mol.%. Thirdly, the melting points of (LiCl-KCl)eut.-xNaCl were confirmed with the OptiMelt™.

Table 2. Salt compositions of LiCl-KCl-NaCl measured.

Salt sample	LiCl (mol.%)	KCl (mol.%)	NaCl (mol.%)
(LiCl-KCl)eut.-0NaCl	59.2	40.8	0
(LiCl-KCl)eut.-3NaCl	57.4	39.6	3
(LiCl-KCl)eut.-5NaCl	56.2	38.8	5
(LiCl-KCl)eut.-9NaCl	53.9	37.1	9
(LiCl-KCl)eut.-12.6NaCl	51.7	35.7	12.6
(LiCl-KCl)eut.-15NaCl	50.3	34.7	15
(LiCl-KCl)eut.-19NaCl	48.0	33.0	19

2.1.1 Differential scanning calorimetry (DSC)

Chloride salts including LiCl (99%, dry, water < 1.0%, Alfa Aesar), NaCl (99.9 %, VWR BDH Chemicals), KCl (99 %, Acro's Organics) were used to synthesize the (LiCl-KCl)eut.-xNaCl salt mixtures. The storage, weighing and mixing of the salts, as well as DSC-crucible sealing, were carried out in a glovebox (GS Glovebox System Technik GmbH, Glovebox Mega 2, O_2 < 0.5 ppm, H_2O < 1 ppm) with ultra-high-purity argon gas (purity > 99.999%). The salt mixtures (~5g for one batch) were ground in a ceramic mortar for at least 20 minutes by hand into small particles to be homogeneous.

The DSC experiments were carried out with a commercial equipment of DSC 204 F1 Phoenix®, purchased from NETZSCH. This DSC equipment was calibrated with standard materials, including In, Sn, Zn, Bi, CsCl, Benzoic Acid, Biphenyl, and $KClO_4$. The crucible of DSC was made of aluminum, consisting of a lid with a small hole and a base. Before the DSC measurement, the crucibles with lids and bases were weighed and transferred into the glovebox. Subsequently, about 8 mg of (LiCl-KCl)eut.-xNaCl mixtures were weighed and charged into the crucibles. Then the crucibles with salt were sealed by pressing with a toolkit. Afterward, they were transferred from the glovebox into the DSC equipment. In the furnace of DSC, they were heated and cooled at a rate

of 10 K/min under 20 ml/min N_2 sweep gas. Three cycles were performed for each sample with a temperature range between 200 °C and 450 °C in every DSC measurement. In the first cycle, the water existing in the salt samples was released, and the samples became more homogeneous after such a melting/cooling cycle. Hence, the results of the first cycles were discarded, while the second- and third-cycle results were recorded and compared with each other.

2.1.2 Melting point measurement apparatus (OptiMelt™)

The Automated Melting Point System - OptiMelt™ (MPA 100, Stanford Research Systems) is an optical melting point measurement equipment employed to verify the melting point of salt samples obtained from DSC. More details on OptiMelt™ could be found in our previous work [16]. Although a result from OptiMelt™ is not as accurate as DSC for measuring melting points, the melting process of salt samples can be visually observed with a magnifier window and recorded with a built-in optical camera. The experiments with this apparatus were implemented in the glovebox.

The salt samples consistent with DSC were filled in three-millimeter-thickness capillary tubes and placed into the OptiMelt. Then the salt samples (~ 10 mg) in the capillary tubes were heated with 10 K/min (the same heating rate as DSC) in the temperature interval of 200-400 °C. Three cycles were performed for each salt sample in line with DSC. The melting-process images of the second and third cycles were recorded.

2.2 Exchange reactions of Na with LiCl-KCl-NaCl

A device was designed to study the exchange reactions of Na with LiCl-KCl-NaCl, consisting of a thermocouple, an oven, a glass carbon crucible, and a group of stainless-steel crucibles, as shown in **Fig. 4**. The device was also used in the glovebox. The temperature was measured by a thermocouple immersed in the molten salt and controlled by a PID temperature controller, with a small fluctuation of e.g., ± 1 °C at 450°C. For each experiment, about 50 g (LiCl-KCl)eut. was loaded in the glass carbon crucible as the salt bath to obtain the homogenous temperature for each batch of experiments. Subsequently, the stainless-steel crucibles with 0.8 g sodium metal and 2.6 g (LiCl-KCl)eut.-3NaCl salt samples were inserted into the heated salt bath, when the temperature of the salt bath reached the target temperature.

A pre-experiment was carried out at 400 °C (the lowest temperature of the experiments) to obtain sufficient time for exchange reactions to reach the equilibrium. The compositions of samples extracted after one-hour reaction were consistent with those extracted after two hours. This

suggests that one hour was enough to reach the equilibrium of the reactions. After the pre-experiment, experiments were carried out at 400, 450, and 500 °C. After one-hour reaction, the samples from metal and salt were separately collected by a collector made up of a quartz tube and a suction tip (see **Fig. 4**). Then the samples were transferred with sealed bottles from the glovebox to post-analysis via Ion Chromatography (IC) to determine the compositions of each sample and the equilibrium constants of exchange reactions.

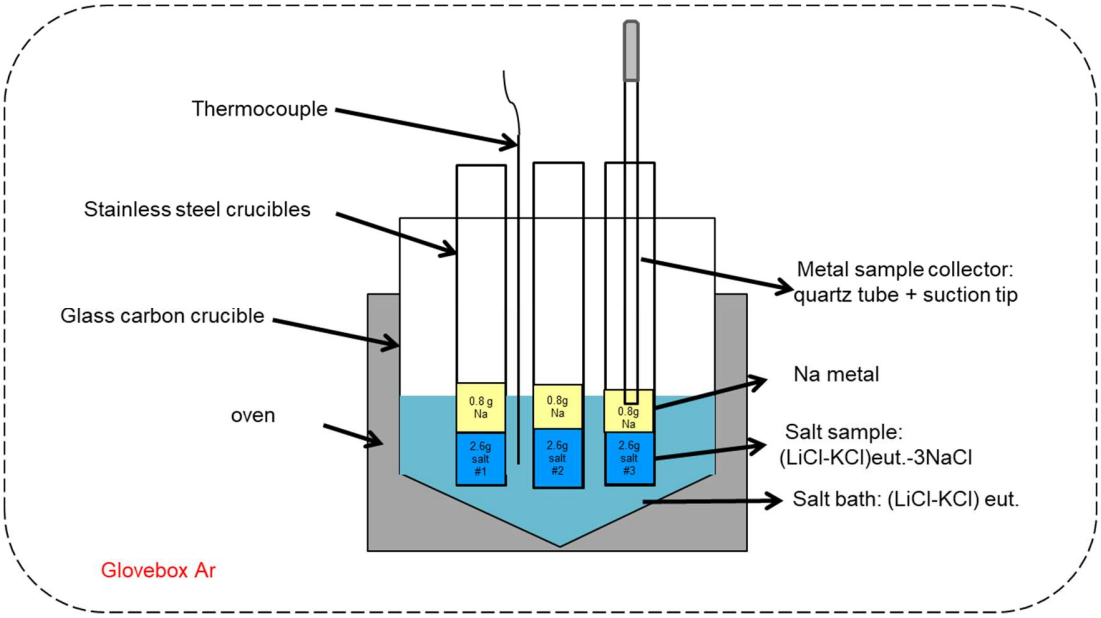

Fig. 4. Sketch of set-up for sodium with LiCl-KCl-NaCl exchange reaction investigation.

For IC measurement, around 100 mg of samples were placed in 500 ml distilled water and measured in a Metrohm model 930 Compact IC Flex (Metrohm, Switzerland). Once exposed to water, the active metal samples reacted violently with water to be water-soluble MOH (M = Na, Li, or K). Ions including Na^+, Li^+, K^+, and Cl^- were measured using a suppressed conductivity detector calibrated according to the lowest signal-to-noise ratio for the ions. Concentrations of the cations (Na^+, Li^+, and K^+) were used to calculate the proportion of Na, Li, and K in the metal and salt phase.

2.3 Battery assembly and testing

The amounts of each component of the electrodes are listed in **Table 3**. The metals used as positive electrode components have high purity (Bi and Sb, 99.99%, from Aladdin). And all cathodes were pre-melted at 650 ℃ for 5 h under argon atmosphere. The (LiCl-KCl)eut.-0NaCl (i.e., eutectic LiCl-KCl salt mixture) was used as the molten salt electrolytes in the test cells, in

order to study the effect of the exchange reactions mentioned above on the battery operation, since in theory a Na-LMB cell with a sodium-ion-free molten salt electrolyte cannot work. All Na-LMB test cells were assembled in the glove box under argon atmosphere and tested by LANHE CT2001A at 450 ℃.

Table 3. The parameters of the Na|LiCl-KCl|Bi_9Sb battery with (LiCl-KCl)eut.-0NaCl electrolyte

	Na	Bi	Sb	Total
Mass (g)	0.85	3.47	0.23	4.55
Density (g/cm^3)	0.968	9.780	6.697	-
Amount of substance (mol)	0.03740	0.01683	0.00187	-
Theoretical capacity (Ah)	-	-	-	0.99
Actual capacity (Ah)	-	-	-	0.60

3. RESULTS AND DISCUSSION

3.1.1 Simulated phase diagram of LiCl-KCl-NaCl

Before the DSC and OptiMelt experiments, the phase diagram of LiCl-KCl-NaCl was simulated with the "Phase Diagram" module of FactSage (Version 7.0). As shown in **Fig. 5**, the simulated phase diagram of this work is in line with the published simulated and experimental phase diagrams in literature. From the simulated and experimental phase diagrams, the minimum liquidus temperature (eutectic melting point) of LiCl-KCl-NaCl is about 350 °C. Moreover, the compositions of liquidus under 375°C are close to the eutectic LiCl-KCl binary system, which contains up to ~13 mol% NaCl.

From the simulated and experimental phase diagrams, this ternary system of LiCl-KCl-NaCl meets at least two features of the pseudo-binary system. Firstly, the lowest melting temperature of this ternary system is near the eutectic LiCl-KCl binary system. Secondly, with the fixed composition of (LiCl-KCl)eut., when the concentration of NaCl is higher than 13 mol.%, this ternary system's melting temperature increases with NaCl concentration. The simulated phase diagram shows that the LiCl-KCl-NaCl is a pseudo-binary system. However, the eutectic composition of this ternary system needs experimental investigation. In the following DSC and OptiMelt experiments, with the fixed eutectic composition of LiCl and KCl (59.2:40.8 in molar

fraction), six proportions for NaCl were set from 0 to 19 mol% in order, as shown on the red line in **Fig. 5**.

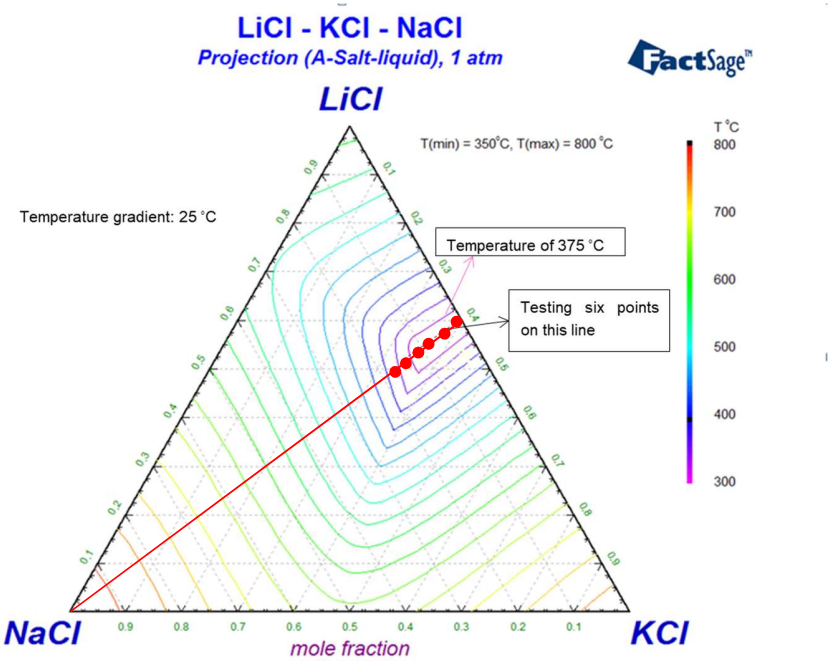

Fig. 5. Phase diagram of the liquidus line of the system LiCl-KCl-NaCl simulated by FactSage.

3.1.2 DSC measurements to determine melting point and eutectic composition

Fig. 6 (a) and **(b)** show the DSC curves of (0-19)NaCl-(LiCl-KCl)eut. salt mixtures. The important parameters for a studied salt sample include the melting peak's onset and end temperature, extrapolated onset (in short: onset), and end temperature of crystallization peak. Some distinctive secondary peaks can be observed in the crystallization process of samples containing > 9 mol.% NaCl in **Fig. 6 (b)**, which is also recorded as an essential parameter. All the parameters obtained from experiments are summarized in **Table 4**. According to DIN EN ISO 11357-1:2010-03 (a standard of DSC) [29], the extrapolation onset point is the intersection of the extrapolation baseline and the inflection tangent line at the beginning of the melting peak. The extrapolation onset point is defined as the melting point of the studied salt.

Comparing the DSC results of different salt samples with each other, it is observed that the onset temperatures of samples are slightly declined from 354.8 °C to 352.1 °C, with the concentration of NaCl increasing from 0 to 19 mol.%. In addition, the main-peak height of both melting and crystallization is declined with the increasing NaCl concentration, indicating that the heat absorption and exhaustion during melting and crystallization decrease with the increasing

NaCl concentration. The melting and crystallization were dispersed in other temperature intervals, which can be supported by two pieces of evidence observed from the DSC curves, as shown in **Fig. 6**.

Firstly, a slight bend of the DSC curve for samples with 9 mol.% NaCl shows at the end of the melting peak. The curve bend is more obvious when the concentration of NaCl is more than 9 mol% (e.g., 19 mol.%, see **Fig. 6 (b)**). This indicates that the melting process extends when NaCl concentrations are higher than 9 mol.%. Secondly, there exist secondary peaks on cooling curves at a higher temperature than the main crystallization peak at about 350°C, when the samples contain >9 mol. % NaCl (see **Fig. 6 (b)**). The DSC curves' secondary peaks for samples with 12.6 mol.%, 15 mol.%, and 19 mol.% NaCl are 372.1 °C, 401.5 °C, and 418.1 °C, respectively. The DSC curves support that the melting/crystallization of salt samples were not completed in the main peaks when the concentration of NaCl is higher than 9 mol.% in salt samples. This implies the limit of NaCl-solubility in (LiCl-KCl)eut. is about 9 mol.% at 352 °C. In other words, the eutectic composition of this ternary system is (LiCl-KCl)eut.-9NaCl with a melting temperature of 352 °C.

In the work of (LiCl-KCl)eut.-NaCl by Sridharan et al. [20], it was suggested that even if the NaCl concentration was as high as 30 mol.%, the melting point of LiCl-KCl was not influenced and maintained at ~355 °C. However, this result conflicts with the study by Gutknecht et al. [30] and Sangster et al. [24], in which authors suppose the liquidus temperature of LiCl-KCl-NaCl with 30 mol. % NaCl was as high as ~500 °C. In our study, the melting process of samples with > 9 mol.% NaCl is seen as a continuous process after the end of the prominent peak, in which slight but not negligible bends can be observed, as shown in Fig. 6 (b). Moreover, a secondary peak can be observed at higher temperatures, which other researchers may ignore, such as Sridharan et al. [20]. In order to confirm the continuous melting process after the prominent peak, the experiments were carried out on OptiMelt.

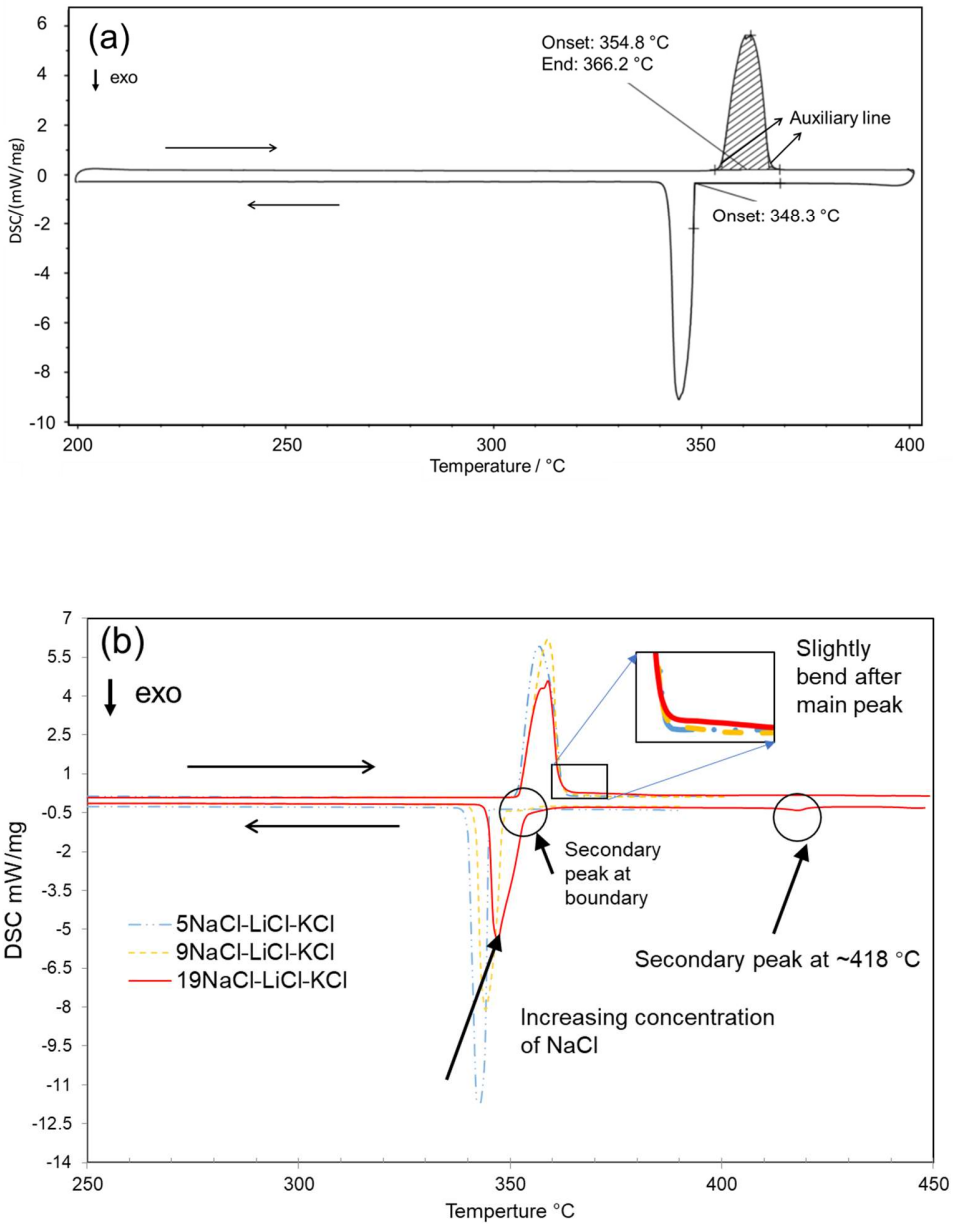

Fig. 6 DSC curves: (a) for 0NaCl-(LiCl-KCl)eut. with peak analysis showing the heating cycle at the top and the cooling cycle at the bottom, (b) for samples with increasing NaCl concentration from 5 to 19 mol%. The DSC curves were tested for three cycles in the temperature range 200–450 °C and heating rate of 10 K/min. Only the second cycle in each DSC test is shown, as the curve of the first cycle contains water release and third cycle is almost identical. In (a), onset temperatures of melting and endset temperatures of crystallization in this work are the extrapolated onset and endset. The auxiliary line shows the drawing method of extrapolated onset and endset.

Table 4. Representative data from DSC curve of LiCl-KCl-NaCl system.

Salt	Onset temperature of melting main peak °C	Onset temperature of crystallization main peak °C	Temperature of secondary peak °C
(LiCl-KCl)eut.-0NaCl	354.8	348.3	None
(LiCl-KCl)eut.-5NaCl	351.9	344.6	None
(LiCl-KCl)eut.-9NaCl	352.4	348.3	On boundary
(LiCl-KCl)eut.-12.6NaCl	352.1	351.3	372.1
(LiCl-KCl)eut.-15NaCl	352.1	352.9	401.5
(LiCl-KCl)eut.-19NaCl	352.1	353.6	418.1

3.1.3 OptiMelt^{TM} results and comparison with DSC

As shown in **Fig. 7**, when the concentration of NaCl is < 9 mol%, the melting process started at ~358 °C and was completed at ~360 °C. The melting of samples with 5 mol. % NaCl and 9 mol. % NaCl was slightly faster than that of samples with 0 mol. %NaCl, consisting with that the melting point of (LiCl-KCl)eut.-0NaCl is marginally higher than that of (LiCl-KCl)eut.-5NaCl and (LiCl-KCl)eut.-9NaCl (as shown in **Table 4**, 355 °C vs. 352 °C).

When the concentration of NaCl is > 9 mol %, as shown in **Fig. 8**, some dispersive particles can still be observed over 370 °C in samples with 15 mol. % and 19 mol. % NaCl. During the heating process, the particles dissolved gradually into the molten salt. The particles could be NaCl or NaCl-rich crystals, as the thickness of dispersive particles increases with NaCl concentration. The particle dissolution observed in the OptiMelt experiments is consistent with the bends observation from DSC curves after the end of the main peak.

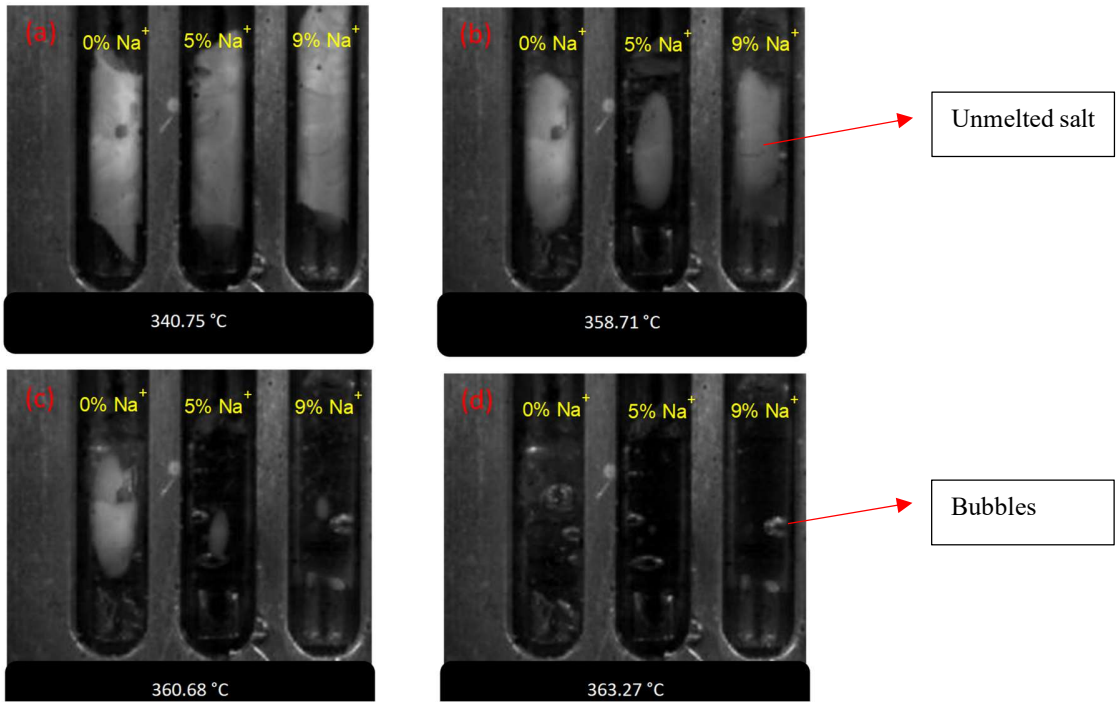

Fig. 7. OptiMelt results of LiCl-KCl-NaCl system. The NaCl concentrations of samples in capillary are 0 mol% (left), 5 mol% (center) and 9 mol% (right), respectively. Temperatures for each photo are 340.75 °C (a), 358.71 °C (b), 360.68 °C (c), 363.27 °C (d). Heating rate: 10K/min.

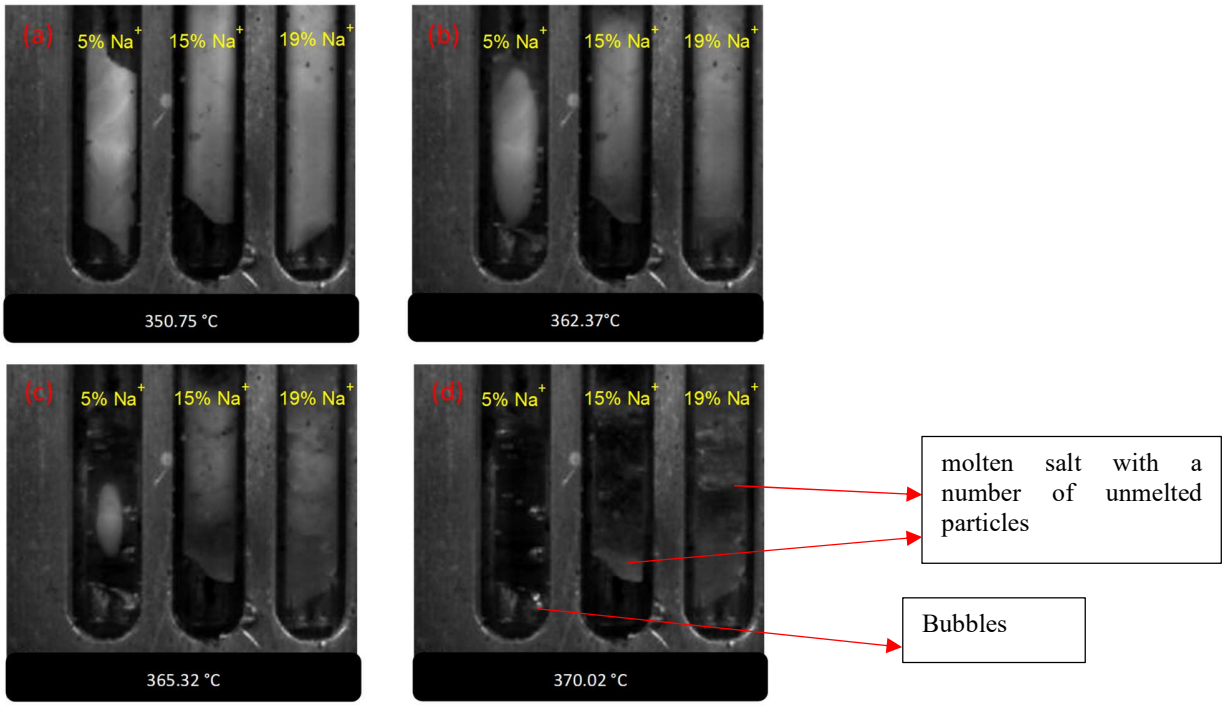

Fig. 8. OptiMelt results of LiCl-KCl-NaCl system. The NaCl concentrations of samples in capillary are 5 mol%(left), 15 mol%(center), and 19 mol% (right), respectively. Temperatures for each photo are 350.75 °C (a), 362.37 °C (c), 365.32 °C (c), and 370.02 °C (d). Heating rate: 10K/min.

3.2 Exchange reactions between Na-anode and LiCl-KCl-NaCl electrolyte

When the reaction in **Eq. 1** happens, $\Delta_r G^\circ$ is equal to $-RTlnK_{eq}$ as shown in **Eq. 2**.

$$\Delta_r G^\circ = -RTlnK_{eq} \quad \textbf{Eq. 2}$$

where

$\Delta_r G^\circ$ is the reaction Gibbs free energy of exchange reactions in J/mol;

R is the universal gas constant (8.314 J/(K·mol));

T is the absolute temperature (K);

K_{eq} is equilibrium constant (-).

The $\Delta_r G^\circ$ can be deduced from **Eq. 3**, that is, the difference of Gibbs free energy of formation of A^+ and B^+ with chloride anion at a specific temperature (e.g., 450 °C).

$$\Delta_r G^\circ = \Delta_{fA} G^\circ - \Delta_{fB} G^\circ \quad \textbf{Eq. 3}$$

where $\Delta_{fA} G^\circ$ and $\Delta_{fB} G^\circ$ (J/mol) are the Gibbs free energy of formation of ACl and BCl, respectively. When the Gibbs free energy of formation of A^+ ($\Delta_{fA} G^\circ$) is higher than that of B^+ ($\Delta_{fB} G^\circ$), the $\Delta_r G^\circ$ in **Eq. 2** is higher than zero. In other words, the equilibrium constant of reaction K_{eq} should be smaller than one. In some practical cases of LMBs with the pure A as the staring anode, the concentration or activity of A^+ can be smaller than that of B^+, as shown in **Eq. 4**.

$$K_{eq} = \frac{a_{(B)} \cdot a_{(A^+)}}{a_{(B^+)} \cdot a_{(A)}} \quad \textbf{Eq. 4}$$

where *a* is the activity of each component in mol.%.

For example, in our previous study, the Na-LMBs were assembled with pure Na sodium as anode and only 5 mol.% NaCl in the electrolyte, which is considerably lower than LiCl and KCl [17]. Hence, the exchange reactions between Na and LiCl-KCl could be a noticeable phenomenon. A series of experiments were carried out as introduced in **Section 2.2** to obtain the detailed parameters of these exchange reactions. The metal- and salt-phase samples were extracted when reactions

between the liquid sodium and (LiCl-KCl)-3NaCl molten salt reached equilibrium at 400 °C, 450 °C, and 500 °C, respectively. IC is used to analyze the composition of each sample and determine the equilibrium constants of these exchange reactions.

3.2.1 Concentration of each components before and after exchange reaction

For either salt or metal samples, the concentrations of ions, including Li^+, K^+, Na^+ cations, and Cl^- anion, were measured by IC after dissolving in distilled water. Under ideal conditions, the OH^- should be the single anion for the metal sample dissolved in water, while Cl^- should be the single anion for the salt sample. However, salt mixed in metal samples and metal mixed in salt samples might exist. For metal samples, the concentration of Cl^- anion can be used to measure salt impurity mixed during the sample extraction. The difference between total cations and Cl^- can be used for salt samples to measure the metal impurity mixed during sample extraction. The IC results show that the concentrations of Cl^- in metal samples were always under the measurement limitation of IC (< 0.1 mg/L), indicating that very little salt impurity exists in the metal phase, i.e., the concentrations of Cl^- in salt samples were significantly smaller than that of total cations. Moreover, some bubbles were observed during the salt samples dissolving in water, most likely hydrogen because of metal impurities reacting with the water. This implies that the samples of salt mixed several metal impurities, leading to considerably high error. Therefore, the analysis and calculation on are based on the metal samples' IC data, and the salt samples' results are abandoned.

Table 5 and **Table 6** show the composition of the metal and salt phases at the beginning and the end of exchange reactions, respectively. After one-hour contact with molten (LiCl-KCl)eut.-3NaCl to reach the reaction equilibrium, the concentration of Na in the metal phase decreased from 100 mol.% to ~92 mol.%, while the concentration of Li and K increased from 0 to ~7 mol.% and ~1 mol.%, respectively. This proves that the exchange reactions of Na with LiCl and KCl are available at a temperature of 400 - 500 °C. The salt compositions were also changed. For example, the composition of the salt mixture has changed from 57.4 mol.% LiCl-39.6 mol.% KCl-3 mol.% NaCl to 52.2 mol.% LiCl-39.0 mol.% KCl-8.8 mol.% NaCl at 400 °C.

Moreover, the same parameters with experiments were typed in FactSage “Equilib” module, and the compositions of each component were output. As shown in **Fig. 9**, according to the results of FactSage, the equilibrium composition of the metal phase was 92.65 mol.% Na-7.35 mol.% Li-0 mol.% K, while the salt phase was 52.5 mol.% LiCl – 39.56 mol.% KCl – 7.98 mol. % NaCl at

400 °C. Although the simulated results from FactSage show neglectable reaction between Na and KCl, the results of Na reacting with LiCl from simulation and experiment are consistent.

Table 5. Composition of each phase before exchange reactions.

Nr.	Temperature °C	Metal and salt samples in crucible (g)		Salt phase composition (mol.%)		
		Na	(LiCl-KCl)eut.-3NaCl	LiCl	KCl	NaCl
1	400	0.716	2.67	57.4	39.6	3
2	450	0.723	2.67	57.4	39.6	3
3	500	0.725	2.67	57.4	39.6	3

Table 6. Composition of each phase after exchange reactions (equilibrium).

Nr.	T °C	Concentration of each elements in metal sample measured by IC (mg/L)				Metal phase composition calculated from IC results (mol.%)			Salt phase composition, deduced from metal phase (mol.%)		
		Li	Na	K	Cl	Na	Li	K	LiCl	KCl	NaCl
1	400	2.62	98.14	1.60	<0.1	91.1	8.0	0.9	52.2	39.0	8.8
2	450	2.07	84.12	1.78	<0.1	91.4	7.5	1.1	52.5	38.9	8.6
3	500	1.59	84.32	2.32	<0.1	92.7	5.8	1.5	53.6	38.6	7.8

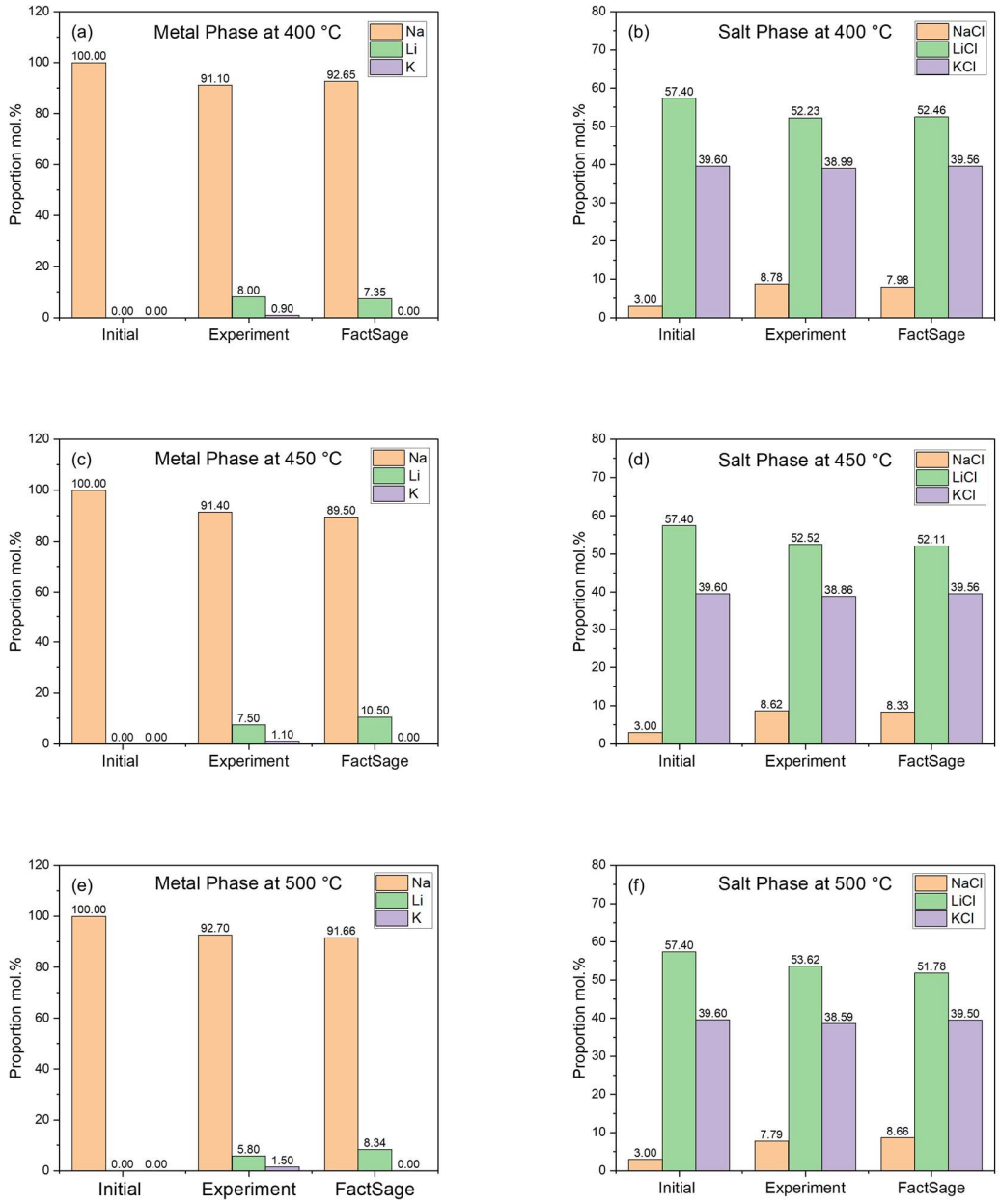

Fig. 9. Comparison of experimental and simulated equilibrium metal and salt phase compositions at 400, 450 and 500 °C. (a), (c), and (e) show the proportion of Na, Li, K metal in the metal phases, while (b), (d9, and (f) show the compositions of salt phases.

3.2.2 Thermodynamic analysis of exchange reactions

In some thermodynamic databases, e.g., Ellingham Diagrams [31] and thermochemical data of pure substances [32], the Gibbs formation free energy of LiCl, KCl, and NaCl can be queried at corresponding temperature. The reaction Gibbs free energy of A metal (e.g., Na) with BCl (e.g., LiCl) can be calculated with the different formation Gibbs free energy between ACl and BCl (see

Eq. 3). In addition, the Gibbs formation free energy can also be extrapolated from electromotive force (EMF) of each metal element in its molten chloride salt [33], as shown in **Eq. 5.**

$$\Delta_r G^\circ = -\Delta E^\circ \cdot F \qquad \textbf{Eq. 5}$$

where ΔE° is the difference of ACl and BCl theoretic electromotive forces (EMFs) in Volt.

In our study, the concentrations of each component at equilibrium were measured, which can be used to calculate the Gibbs free energy of reactions (assume the activity is equal to concentration), as shown in **Eq. 2** and **Table 7**. It makes sense to compare the Gibbs free energy of reactions based on our experiments and thermodynamic data from the literature [31-33], as shown in **Fig. 10**.

Table 7. Calculated K_{eq} and $\Delta_r G^\circ$ of Na with LiCl and Na with KCl based on experimental results.

Nr.	T °C	K_{eq} (Na and Li^+), assuming concentration is equal to activity	K_{eq} (Na and K^+), assuming concentration is equal to activity	$\Delta_r G^\circ$ (Na + LiCl) kJ/mol	$\Delta_r G^\circ$ (Na + KCl) kJ/mol
1	400	0.01476	0.00222	23.59	34.18
2	450	0.01347	0.00267	25.89	35.62
3	500	0.00910	0.00327	30.20	36.78

All of the $\Delta_r G^\circ$(LiCl with Na and KCl with Na) show only a slight difference from our work to literature data (< 30 kJ/mol) [31-33]. The difference could result from two factors. Firstly, the status of both reactants and products is not included in the calculation. The status of reactants, for example, LiCl and KCl in our study, were liquid at 400 °C because of eutectic, while in the literature, both LiCl and KCl are solid at 400 °C due to the temperature of 400 °C is smaller than the melting point of pure LiCl (m.p. = 605 °C) and KCl (m.p. = 770 °C). Secondly, the activities of the reactants and products are simplified to the concentrations of the reactants and products which may lead to the error of equilibrium constant (K_{eq}) and $\Delta_r G^\circ$.

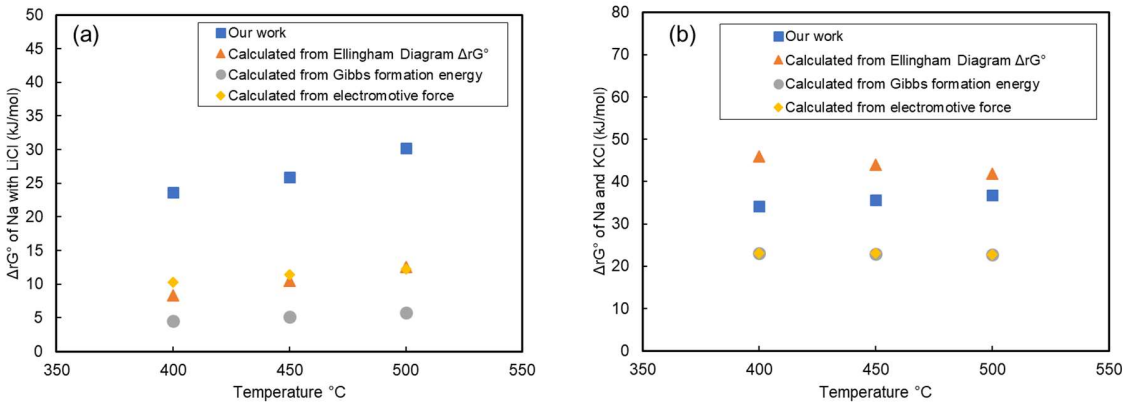

Fig. 10. Comparison of experimental (a) $\Delta_r G^\circ$(Na + LiCl) and (b) $\Delta_r G^\circ$(Na + KCl) with calculation data based on literature.

3.3 Discussion on LiCl-KCl-NaCl as the electrolyte of Na-LMBs

3.3.1 Influence of exchange reactions on Na-LMB

In our previous work, Zhou et al. [17] tested the Na| LiCl-NaCl-KCl (59:5:36 mol%) |Bi_9Sb cells at 450 °C, which reached a high energy efficiency of approximately 80 %, a coulombic efficiency of 97% and almost no storage capacity loss after 700 cycles (estimated more than 15 000 cycles in lifetime). This proved the feasibility of the multi-cationic electrolyte LiCl-KCl-NaCl used in Na-LMB. In addition, it was pointed out that the low melting point of the electrolyte leads to low operating temperature and further leads to low self-discharge of batteries. In the previous study, the Na-LMBs at 450°C with 5 mol.% NaCl in electrolyte showed better performance than that with 9 mol. % NaCl in electrolyte [17]. This phenomenon can be explained in two directions.

Firstly, the better performance of 5 mol.% NaCl Na-LMB can be explained based on the pseudo-binary system. During the discharge of batteries, the sodium metal converts to Na^+ at the interface of the anode and electrolyte. The localized NaCl-rich layer could be generated due to concentration polarization, as shown in **Fig. 11 (a)**. In some exceptional conditions, such as the rapid discharge of batteries, the NaCl concentration at the boundary can surpass the solubility limit, leading to precipitation of the Na-rich layer. This results in a severe increase in battery internal resistance and a reduction in efficiency. The electrolyte containing 5 mol.% NaCl is farther from the solubility limit (about 20 mol.% at 450°C) than that with 9 mol.% NaCl, so the NaCl can be dissolved into the electrolyte faster, reducing the possibility of the formation NaCl-rich layer.

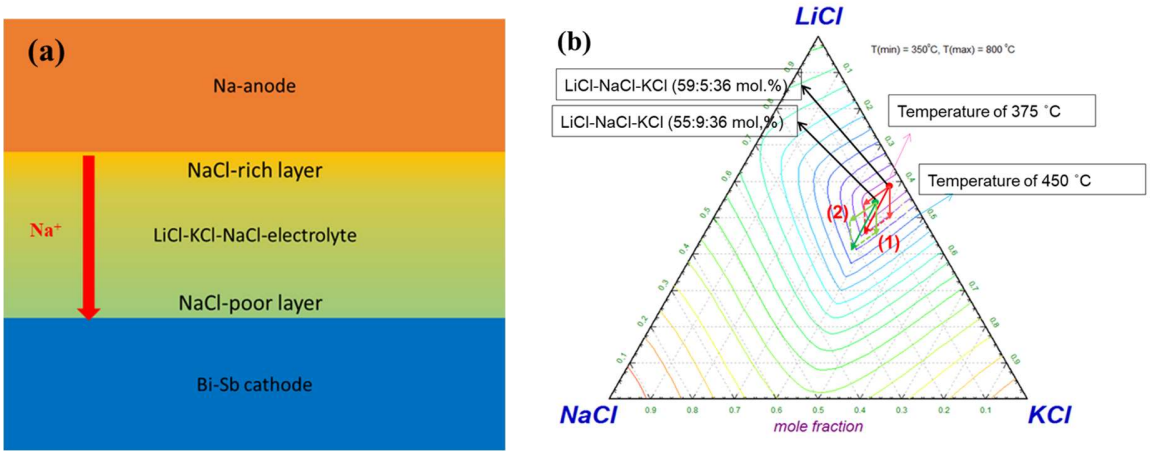

Fig. 11. (a) Schematic diagram of the NaCl-rich layer in electrolyte during rapid discharge. (b) Schematic of composition drifting because of NaCl generated and LiCl consumed during exchange reactions.

Secondly, the better performance of 5 mol.% NaCl Na-LMB can be explained based on the exchange reactions. As discussed above, the exchange reactions will change the electrolyte composition and melting temperature, significantly influencing battery performance. On the one hand, the ratio between LiCl and KCl deviates from the eutectic composition (Direction 1 in **Fig. 11 (b)**). On the other hand, the generated NaCl from exchange reactions increases NaCl concentration (Direction 2 in **Fig. 11 (b)**). As can be seen, the composition shifting of the electrolyte destroys the pseudo-binary system, further leading to a significant increase in the melting point. For the electrolyte with 9 mol.% (the green arrow in **Fig. 11 (b)**), this shifting of salt composition can lead to much higher melting point (close to 450°C) than that that with 5 mol.% NaCl (the red arrow in **Fig. 11 (b)**). During discharging, it would be more sensitive to form a NaCl-rich layer on the boundary, leading to the bad performance of Na-LMBs.

3.3.2 Battery test results and discussion

As shown in **Fig. 12**, a Na-LMB with LiCl-KCl electrolyte cycle plot is displayed with charge capacity, discharge capacity, and coulombic efficiency. The test of this battery can be divided as two phases, as shown in **Fig. 12**. During the first phase (Phase I), the capacity of this battery increased from zero to ~ 0.7 Ah, indicating that the exchange reactions occurred between Na-anode and LiCl-KCl and generated the effectively conductive ions (Na^+) in the molten salt electrolyte. In addition, the coulombic efficiency of some cycles was larger than 100 %, resulting from the additional electrons transferring also because of the exchange reactions. After the exchange reactions phase, the battery reached a relatively steady-state step by step, as shown in the second phase (Phase II) of **Fig. 12**. In the second phase, the battery runs with ~95 % coulombic efficiency

for up to 255 cycles without degradation, indicating a longer service life than other successful LMBs [3, 9, 17].

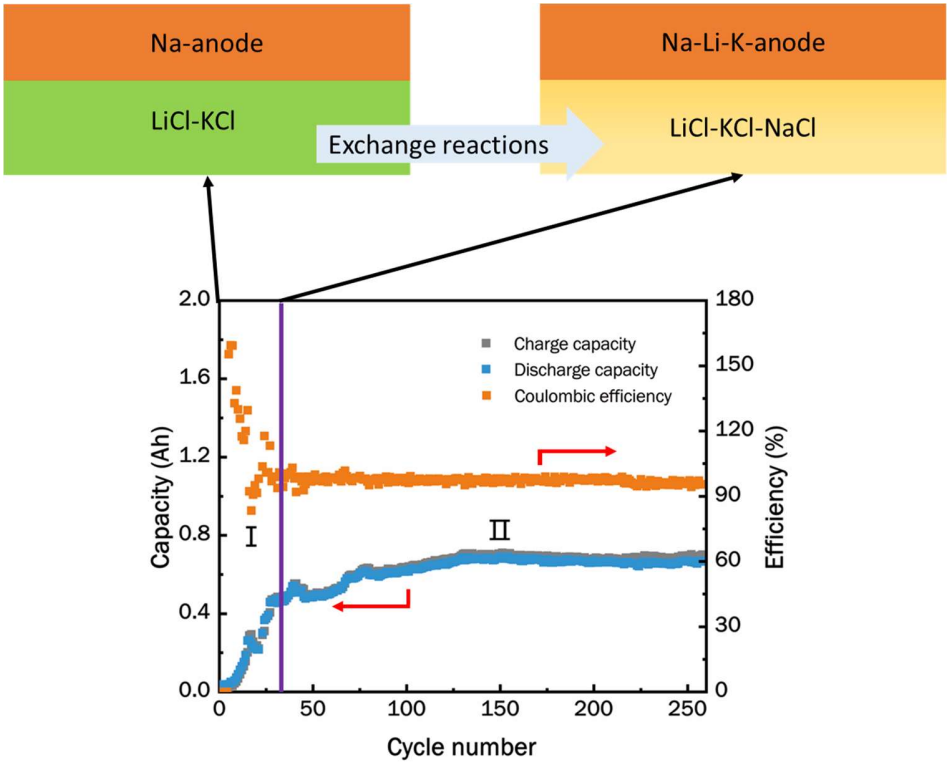

Fig. 12. Test results of the Na-LMB with a LiCl- KCl (59:41 mol%) electrolyte. Charge capacity, discharge capacity, and coulombic efficiency as a function of cycle number, and the theoretical capacity is 1Ah. The test of this battery can be divided into two phases: exchange reaction phase and equilibrium phase.

3.3.3 Effective ion conductivity

With the method used in our previous work on LiI-KI-NaI [16], the effective conductivity of the Na+ ion is estimated by calculation. To our best knowledge, it is a lack of experimental data on the effective conductivity of Na^+ ion in molten LiCl-KCl-NaCl. Same as the iodide conductivity estimation, two hypotheses are suggested:

(1) The Na^+ ions are the only effective ions for conductivity of the molten LiCl-KCl-NaCl electrolyte,

(2) The Na^+ conductivity relates linearly to the concentration of Na^+ ions, according to Kohlrausch's law for independent migration of ions [34].

In contrast to LiI-KI-NaI, the total conductivity of LiCl-KCl-NaCl (S/cm) is available in the literature [25], as shown in **Eq. 6**.

$$\kappa_{total} = -3.80334 + 0.007595 \times T \quad \textbf{Eq. 6}$$

where T is the absolute temperature (K).

Thus, the effective conductivity of LiCl-KCl-NaCl with different Na^+ concentrations can be estimated according to **Eq. 7**.

$$\kappa_{eff} = \kappa_{total} \times c_{Na^+} \quad \textbf{Eq. 7}$$

where the temperature dependence of the conductivity of LiCl-KCl-NaCl is given by **Eq. 6** in S/cm, and the c_{Na^+} is the concentration of Na^+ ions in electrolyte in mol.%.

Moreover, it is reasonable to suppose that the Na^+ ions are the only effective ions for conductivity. In this work, the tests with the cell with a LiCl-KCl electrolyte show that the capacity was almost zero in the first cycle (see **Fig. 12**), when the exchange reactions did not occur. The cell capacity increased with the increasing cycle number (i.e., the operating time), implying the formation of NaCl in the molten salt electrolyte by the exchange reactions.

As shown in **Fig. 13**, the estimated effective conductivity of LiCl-KCl-NaCl with 3-9 mol.% NaCl is higher than 40 mS/cm. In the battery test, it was no evidence that the effective conductivity could be the restriction of Na-LMBs with only 5 mol.% NaCl in the starting molten salt electrolyte [17]. Using the equilibrium constants in **Section 3.2**, it is estimated that there was more than 10 mol.% NaCl in the molten salt electrolyte in the test cell [17] and thus the estimated effective conductivity could be higher than 150 mS/cm at 450°C.

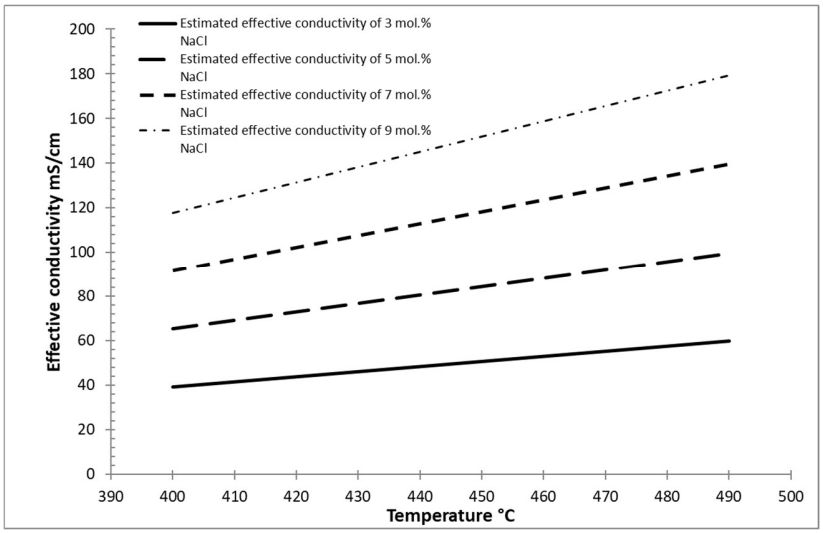

Fig. 13. Estimated effective conductivity of LiCl-KCl-NaCl with 3–9 mol% NaCl at 400-500 °C.

4. CONCLUSIONS AND OUTLOOK

In this work, the LiCl-KCl-NaCl molten salt electrolytes for Na-LMBs were systematically investigated, including their compatibility with the Na anode (exchange reactions) and properties such as melting temperature, effective conductivity. The main conclusions can be summarized as follow:

1. According to simulated results from FactSage and experimental results from DSC and OptiMelt, the LiCl-KCl-NaCl ternary system can be seen as the pseudo-binary system, in which the (LiCl-KCl)eut. is seen as solvent and NaCl is seen as solute.
2. The eutectic composition of LiCl-KCl-NaCl is 53.9 - 37.1 - 9 mol. % with a melting point of about 350 °C. In other words, the solubility of NaCl in (LiCl-KCl)eut. is 9 mol.% at the eutectic melting temperature of about 350 °C. The solubility of NaCl in (LiCl-KCl)eut. increases with temperature.
3. The estimated effective conductivities (i.e., Na-ion-conductivities) of (LiCl-KCl)eut.-NaCl with more than 3 mol.% NaCl are >40 mS/cm. No restriction by Na-ion-conductivity was observed in the battery test with such LiCl-KCl-NaCl molten salt electrolytes at 450°C.
4. Although the reactivities of Li and K are higher than Na, the exchange reactions of Na with LiCl and KCl are proved to occur. Based on IC measurements, equilibrium constants of Na reacting with LiCl are 0.01476, 0.01347, and 0.0091 at 400 °C, 450 °C,

and 500 °C, respectively, while the equilibrium constants of Na reacting with KCl are 0.00222, 0.00267, and 0.00327 at 400 °C, 450 °C, and 500 °C, respectively.

5. The exchange reactions could change the composition of the molten salt electrolyte, further leading to change of the melting temperature of the electrolyte and worse performance of the Na-LMBs. The determined equilibrium constants of Na reacting with LiCl and KCl could be used to design the LiCl-KCl-NaCl molten salt electrolyte for Na-LMB for better energy storage performance.
6. A one ampere-hour (Ah) Na-LMB test cell with LiCl-KCl molten salt electrolyte was built based on the findings in this work and shows promising energy storage performance (~95 % coulombic efficiency, >60% of energy efficiency). Moreover, it confirms the exchange reactions.
7. The findings on the multi-cationic molten salt electrolyte in this work could support further development of the liquid metal batteries.

ACKNOWLEDGEMENT

This research has been performed within the DFG-NSFC Sino-German project (DFG Project Member 411450529): 'Study on Corrosion Control and Low-Temperature Electrolytes for Low-Cost Na-based Liquid Metal Batteries', which is funded by Deutsche Forschungsgemeinschaft (DFG) and National Natural Science Foundation of China (NSFC, Grant No. 52177215, 51861135315). The authors would like to thank their colleagues Markus Braun, and Andrea Hanke at the DLR-Institute of Engineering Thermodynamics for their support.

REFERENCE

1. Kim, H., et al., *Liquid Metal Batteries: Past, Present, and Future.* Chemical Reviews, 2013. **113**(3): p. 2075-2099.
2. Zhang, S., et al., *Liquid metal batteries for future energy storage.* Energy & Environmental Science, 2021. **14**(8): p. 4177-4202.
3. Wang, K., et al., *Lithium–antimony–lead liquid metal battery for grid-level energy storage.* Nature, 2014. **514**(7522): p. 348-350.
4. Bradwell, D.J., et al., *Magnesium–Antimony Liquid Metal Battery for Stationary Energy Storage.* Journal of the American Chemical Society, 2012. **134**(4): p. 1895-1897.
5. Li, H., et al., *Tellurium-tin based electrodes enabling liquid metal batteries for high specific energy storage applications.* Energy Storage Materials, 2018. **14**: p. 267-271.
6. Li, H., et al., *High Performance Liquid Metal Battery with Environmentally Friendly Antimony–Tin Positive Electrode.* ACS Applied Materials & Interfaces, 2016. **8**(20): p. 12830-12835.
7. Cui, K., et al., *Low-Temperature and High-Energy-Density Li-Based Liquid Metal Batteries Based on LiCl–KCl Molten Salt Electrolyte.* ACS Sustainable Chemistry & Engineering, 2022. **10**(5): p. 1871-1879.

8. Blanchard, A., *Enabling multi-cation electrolyte usage in LMBs for lower cost and operating temperature*. 2013, Massachusetts Institute of Technology.
9. Ouchi, T., et al., *Calcium-based multi-element chemistry for grid-scale electrochemical energy storage.* Nature Communications, 2016. **7**(1): p. 10999.
10. Kim, H., et al., *Calcium–bismuth electrodes for large-scale energy storage (liquid metal batteries).* Journal of Power Sources, 2013. **241**: p. 239-248.
11. Xu, J., et al., *Na-Zn liquid metal battery.* Journal of Power Sources, 2016. **332**: p. 274-280.
12. Weier, T., et al., *Liquid metal batteries - materials selection and fluid dynamics.* IOP Conference Series: Materials Science and Engineering, 2017. **228**: p. 012013.
13. ESJ. *https://www.energystoragejournal.com/ambri-secures-144-million-to-commercialize-and-expand/*. 2021 [cited 2022.06.23].
14. Cairns, E.J., et al., *GALVANIC CELLS WITH FUSED-SALT ELECTROLYTES.* 1967, Argonne National Lab. (ANL), US, Technical Report ANL-7316. https://doi.org/10.2172/4543889.
15. Ding, W., A. Bonk, and T. Bauer, *Corrosion behavior of metallic alloys in molten chloride salts for thermal energy storage in concentrated solar power plants: A review.* Frontiers of Chemical Science Engineering, 2018. **12**(3): p. 564-576.
16. Gong, Q., et al., *Molten iodide salt electrolyte for low-temperature low-cost sodium-based liquid metal battery.* Journal of Power Sources, 2020. **475**: p. 228674.
17. Zhou, H., et al., *A sodium liquid metal battery based on the multi-cationic electrolyte for grid energy storage.* Energy Storage Materials, 2022. **50**: p. 572-579.
18. FactSage. *https://www.crct.polymtl.ca/fact/phase_diagram.php?file=KCl-LiCl.jpg&dir=FTsalt*. [cited 2022 2022.06.28].
19. Basin, A.S., et al., *The LiCl-KCl binary system.* Russian Journal of Inorganic Chemistry, 2008. **53**(9): p. 1509-1511.
20. Sridharan, K., et al., *Thermal Properties of LiCl-KCl Molten Salt for Nuclear Waste Separation*. 2012, Office of Scientific and Technical Information (OSTI).
21. Fusselman, S.P., et al., *Thermodynamic Properties for Rare Earths and Americium in Pyropartitioning Process Solvents.* Journal of The Electrochemical Society, 1999. **146**(7): p. 2573-2580.
22. Ghosh, S., et al., *Investigation on the Phase Diagram of LiCl-KCl-NdCl3 Pseudo-Ternary System.* Journal of Phase Equilibria and Diffusion, 2018. **39**(6): p. 916-932.
23. Nakamura, K. and M. Kurata, *Thermal analysis of pseudo-binary system: LiCl · KCI eutectic and lanthanide trichloride.* Journal of Nuclear Materials, 1997. **247**: p. 309-314.
24. Songster, J. and A.D. Pelton, *Thermodynamic calculation of phase diagrams of the 60 common-ion ternary systems containing cations Li, Na, K, Rb, Cs and anions F, Cl, Br, I.* Journal of Phase Equilibria, 1991. **12**(5): p. 511-537.
25. Janz, G.J., et al., *Physical properties data compilations relevant to energy storage, 2. Molten salts: Data on single and multi-component salt systems.* Nasa Sti/recon Technical Report N, 1979. **80**: p. 10643.
26. Mamiya, M., *The Near-infrared Absorption Spectra of Lanthanide Chlorides Dissolved in Molten LiCl–NaCl–KCl Eutectic.* Bulletin of the Chemical Society of Japan, 1965. **38**(2): p. 178-183.
27. Yanagi, T. and T. Ohkuma, *Behaviors of Impurities in Liquid Sodium, (III).* Journal of Nuclear Science and Technology, 1979. **16**(2): p. 132-136.
28. Bale, C.W., et al., *FactSage thermochemical software and databases.* Calphad, 2002. **26**(2): p. 189-228.
29. Normung, D.I.f., *Plastics - Differential scanning calorimetry (DSC) - Part 1: General principles* in *DIN EN ISO 11357-1:2010-03*. 2010, Beuth: German.
30. Gutknecht, T.Y., G.L. Fredrickson, and V. Utgikar, *Thermal Analysis of Surrogate Simulated Molten Salts with Metal Chloride Impurities for Electrorefining Used Nuclear Fuel*. 2012, Idaho National Laboratory (INL).
31. Howard, S.M., *Ellingham diagrams.* SD School of Mines and Technology, 2006.

32. Barin, I. and G. Platzki, *Thermochemical data of pure substances*. Vol. 304. 1989: Wiley Online Library.
33. Hamer, W.J., M.S. Malmberg, and B. Rubin, *Theoretical Electromotive Forces for Cells Containing a Single Solid or Molten Chloride Electrolyte.* Journal of The Electrochemical Society, 1956. **103**(1): p. 8.
34. Castellan, G., *Physical chemistry: the elecfricul current in ionic rolutions*. 1983, Addison-Wesley Publishing Co., Reading, MA.